



# The oscillatory nature of the geomagnetic field during reversals

Clément Narteau<sup>a,\*</sup>, Jean-Louis Le Mouél<sup>b</sup>, Jean-Pierre Valet<sup>c</sup>

<sup>a</sup> *Laboratoire de Dynamique des Fluides Géologiques, Institut de Physique du Globe de Paris, 4, Place Jussieu, Paris, Cedex 05, 75252, France*

<sup>b</sup> *Laboratoire de Géomagnétisme, Institut de Physique du Globe de Paris, 4, Place Jussieu, Paris, Cedex 05, 75252, France*

<sup>c</sup> *Laboratoire de Paléomagnétisme, Institut de Physique du Globe de Paris, 4, Place Jussieu, Paris, Cedex 05, 75252, France*

Received 2 March 2007; received in revised form 6 July 2007; accepted 7 July 2007

Available online 17 July 2007

Editor: R.D. van der Hilst

---

## Abstract

We investigate the phenomenology of reversals predicted by a multiscale  $\alpha\omega$  dynamo model in which a hierarchical structure of length scales accounts for the nature of turbulent thermal convection at a very high Rayleigh number. Cyclones at different length scales contribute to the  $\alpha$ -effect. During polarity chrons, a progressive population inversion invariably yields to a change of sign of the  $\alpha$ -effect which initiates reversals. The dipole weakens and turbulent motions are able to cascade through a wide range of length scales to produce large fluctuations of the  $\alpha$ -effect. These fluctuations (1) reinforce magnetic fields with opposite polarity, or (2) trigger large instabilities in direction and intensity of the dipole. This behaviour is reflected in the real Earth by the existence of chrons and reversals. The simulations also predict different degrees of complexity in the reversal process which depends on the spontaneous change in sign of the  $\alpha$ -effect. The existence of similar oscillations in the detailed reversal records suggests that geomagnetic reversal would result from equivalent underlying mechanisms.

© 2007 Elsevier B.V. All rights reserved.

*Keywords:* geodynamo; reversals; paleointensity

---

## 1. Introduction

The behaviour of the geomagnetic field over geological times, with long periods of stable polarity alternating with fast reversals, is one of the most fascinating phenomena of Earth's Sciences. In the present paper, we will focus on the temporal characteristics of reversals. It is widely accepted that reversals do not last more than a few thousand years (Quidelleur, 2003; Clement, 2004;

Valet et al., 2005), but their spatial and temporal structures are still controversial issues.

Three dimensional simulations of magnetohydrodynamics (MHD) interactions performed by several teams during the last decade yielded very interesting results (e.g. Glatzmaier and Roberts, 1995; Kuang and Bloxham, 1997; Kageyama and Sato, 1997; Olson et al., 1999; Simitsev and Busse, 2005; Christensen and Aubert, 2006). Despite these major advances, it is clear that computer technology still needs to improve considerably before meeting the requirements for a realistic model of the geodynamo (Dormy et al., 2000). Other approaches have been proposed to constrain the mechanism controlling the frequency and characteristics

---

\* Corresponding author.

*E-mail addresses:* [narteau@ipgp.jussieu.fr](mailto:narteau@ipgp.jussieu.fr) (C. Narteau), [lemouel@ipgp.jussieu.fr](mailto:lemouel@ipgp.jussieu.fr) (J.-L. Le Mouél), [valet@ipgp.jussieu.fr](mailto:valet@ipgp.jussieu.fr) (J.-P. Valet).

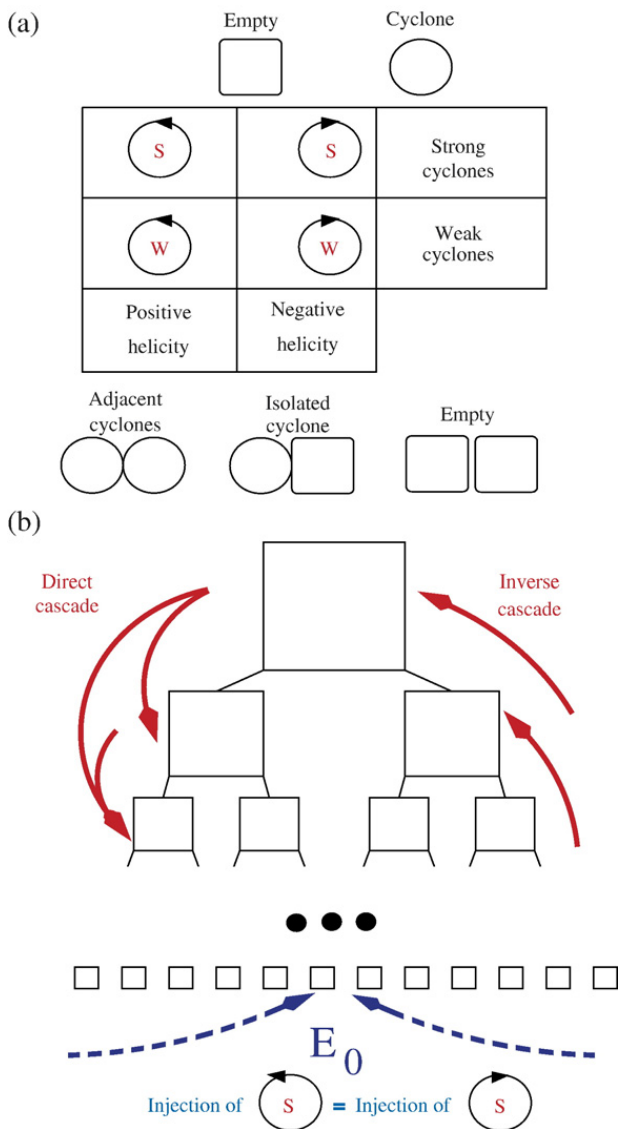


Fig. 1. (a) Different possible states and doublets. There are 5 states. From them, the 10 doublets of adjacent cyclones, 4 doublets of isolated cyclone and 1 empty doublet can be formed. The discrete dynamics is based on nonstationary transition rates between all these doublets, different sets of transitions being related to different physical processes. (b) Hierarchical system with a renormalisation factor  $\mathcal{R} = 2$ . Solid arrows represent the interactions between constituent parts of the system at different length scales (i.e. the cascades). Dashed arrows represent the injection of helicity at the elementary scale of the system. This helical forcing is our control parameter, characterized by a constant rate  $E_0$ , the same for both orientations.

of geomagnetic reversals (Rikitake, 1958; Nozières, 1978; Hide, 1995; Le Mouél et al., 1997; Narteau et al., 2000; Hoyng et al., 2001; Stefani and Gerbeth, 2005). The underlying idea is that some conclusions, even derived from an abstract and schematic modeling, should still remain valid when operating more elaborate models, such as the 3-D MHD simulations mentioned above, and be relevant to the real field.

## 2. Discrete modelling

What are the parameters which drive, at least in a statistical sense, the field behaviour during reversals? In the following we discuss this question, in the frame of a simple abstract model of the dynamo.

### 2.1. The abstract model of turbulence

The present model has been described in Blanter et al. (1999) and Narteau and Le Mouél (2005). We will just recall here the main characteristics which are particularly relevant to the present study.

This multiscale dynamo model is basically a cellular automaton (CA) with a finite number of states designed to represent the statistical properties of a turbulent field within a volume where dynamo action takes place (Blanter et al., 1999). A given cell of the automaton can be in a finite number (5) of states: it can contain a strong or a weak cyclone with positive or negative helicity, or be void (Fig. 1). In order to combine short and long interaction length scales, the automaton is operated on a hierarchy of cells. At a given time step, and for all length scales, a set of transitions modifies the density of all kinds of cell doublets according to a set of rules defined from physical constraints. Stochastic transition rates are the same for both signs of the cyclones (positive and negative helicity), and depend on the energy of the prevailing magnetic field. Four main features are important in the framework of the present study (Fig. 1).

- (1) We assume permanent injection of helicity, the same amount for both signs, characterized by a source term  $E_0$  (a cell of the smallest length scale remains void for a period of time which is in average equal to  $E_0^{-1}$ ).
- (2) We assume permanent relaxation of cyclones at all length scales (strong  $\rightarrow$  weak) and permanent dissipation of helicity at the smallest length scale (weak  $\rightarrow$  zero). This is the sink term which compensates statistically for the source term  $E_0$ .
- (3) There is continuous transfer of helicity from smaller to larger length scales (inverse cascade).
- (4) There is continuous transfer of helicity from larger to smaller length scales (direct cascade).

### 2.2. A simplified $\alpha\omega$ dynamo

Using this model of turbulence as an essential ingredient, we consider an abstract  $\alpha\omega$  dynamo. The basic equations are extremely simplified, but the originality of this dynamo lies in coupling a set of differential

equations with a CA approach, which is known to be relevant for analysing pattern formation, especially in turbulence (Frisch et al., 1986; Chopard and Droz, 1998).

We retain a single poloidal mode  $\vec{B}_S$  and a single toroidal mode  $\vec{B}_T$  varying with time:

$$\vec{B}(\vec{r}, t) = T(t) \vec{B}_T(\vec{r}) + S(t) \vec{B}_S(\vec{r}), \quad (1)$$

where  $t$  is the time,  $\vec{r}$  is the current point and  $T(t)$  and  $S(t)$  may be directly related to both the intensity and the polarity of the toroidal mode, e.g.  $\vec{T}_2^0$ , and of the poloidal mode, e.g. the dipolar mode  $\vec{P}_1^0$  (a mode is a vector field of constant geometry; in usual axisymmetric  $\alpha\omega$  dynamo the poloidal and the toroidal components  $\vec{B}_S$  and  $\vec{B}_T$  are functions of  $\theta, r$ , with  $t, \theta$  being the colatitude).

Here the toroidal field is built from the poloidal field through differential rotation, whereas the poloidal component is built from the toroidal field through some multiscale  $\alpha$ -effect. Our abstract dynamo is then ruled by two differential equations:

$$\frac{\partial T(t)}{\partial t} = -\frac{T(t)}{\Theta_T} + \omega S(t), \quad (2)$$

$$\frac{\partial S(t)}{\partial t} = -\frac{S(t)}{\Theta_S} + \mathcal{H}(t)T(t), \quad (3)$$

where  $\Theta_S$  and  $\Theta_T$  are the diffusive times for the  $S$  and  $T$  components respectively,  $\omega$  is the effect of differential rotation and  $\mathcal{H}(t)$  a multiscale  $\alpha$ -effect defined as

$$\mathcal{H}(t) = \zeta \sum_{k=1}^K \sum_{i=1}^2 \frac{\rho_i(P_i(k, t) - Q_i(k, t)) \chi^k}{N_k}, \quad (4)$$

where  $\mathcal{K}$  is the total number of length scales in the hierarchical system,  $\zeta$  and  $\chi$  are positive constants,  $N_k$  is the total number of cells of the length scale  $k$ ,  $P$  and  $Q$  are the numbers of cyclones of positive and negative helicity respectively; index  $i$  is for strong ( $i=1$ ) and weak ( $i=2$ ) states, with  $0 < \rho_2 \ll \rho_1$ .

Contrarily to  $\omega$  which is a constant in the present model,  $\mathcal{H}$  at a given time depends on the configuration of cyclones at all length scales. This configuration results from the entire history of the cyclone population which is itself controlled by the intensity of the magnetic fields through a feedback mechanism that depends on the magnetic energy  $W(t)$  where  $W(t) = S^2(t) + T^2(t)$ . Essentially, the inverse cascade flow strengthens when  $W$  increases, whereas the direct cascade flow weakens. Hence the feedback mechanism is included in  $\mathcal{H}$ , although the scalar  $\mathcal{H}(t)$  does not describe by itself the state of the model of turbulence at time  $t$ .

The magnitude of the  $\alpha$ -effect during chrons and reversals is not given a priori, but results from the evolution of the cyclone population in the model. The magnetic properties predicted by such agent-based models grow out of the internal dynamics. Thus, there are a variety of possible evolutions from a given state. For example, the  $\alpha$  quenching mechanism is not imposed (e.g. Brandenburg et al., 1989; Hide, 1998), and  $\mathcal{H}$  and  $W$  are not linked by a simple relationship like  $f(W(t), \mathcal{H}(t)) = 0$ . On the contrary, this relationship depends on the history of the model before time  $t$ , and a wide range of behaviours can be observed. In this paper we pay special attention to the phenomenology of reversals derived from the numerical simulations.

### 3. Statistically stable solutions — chrons

Eqs. (2) and (3) are similar (although more simplified) to other sets of partial differential equations used to account for different features of field behaviour during reversals (Hoyng et al., 2001; Stefani and Gerbeth, 2005). The solution of the systems of Eqs. (2) and (3) for an  $\mathcal{H}$ -value not varying in time, denoted as  $\bar{\mathcal{H}}$ , is straightforward; this solution is referred to as  $\bar{S}$ ,  $\bar{T}$ . For the sake of simplicity, we assume

$$\Theta_S = \Theta_T = \Theta = \frac{1}{K},$$

and we have taken  $\Theta = 10$  kyr and  $1/\omega = 5$  kyr in all numerical simulations. For a nontrivial solution  $\bar{S}, \bar{T}, \bar{\mathcal{H}}$  to exist, the condition equation

$$\bar{\mathcal{H}}\omega = \Theta^{-2}$$

is required (assuming  $\omega$  is a constant).  $\bar{\mathcal{H}} > 0$ , since we have chosen  $\omega > 0$ . Then

$$\bar{S} = \bar{\mathcal{H}}\Theta\bar{T}, \quad \bar{S}\bar{T} > 0.$$

The system of Eqs. (2) and (3) is homogeneous for stationary solutions, and  $\bar{S}$  and  $\bar{T}$  are defined within a multiplicative constant. In fact, when the system is working,  $\mathcal{H}$  is always varying, and during chrons,  $\mathcal{H}, S$  and  $T$  fluctuate around their mean value  $\bar{\mathcal{H}}, \bar{S}$ , and  $\bar{T}$ . Due to the feedback mechanism,  $\bar{\mathcal{H}}$  is a function of  $\bar{W} = \bar{T}^2 + \bar{S}^2$  (with all the parameters of the model kept constant). Then the time steady regime, or chron regime,  $\bar{S}, \bar{T}, \bar{\mathcal{H}}$ , is completely defined by the two equations

$$\bar{S} = \bar{\mathcal{H}}\Theta\bar{T}, \quad \text{and} \quad \bar{\mathcal{H}}(\bar{W}) = \frac{1}{\omega\Theta^2}. \quad (5)$$

The last relationship, which is determined empirically indicates that the efficiency of the dynamo characterized by the product  $\bar{\mathcal{H}}\omega$ , just fits the ohmic dissipation characterized by the dissipative time  $\Theta$ .

#### 4. Fluctuations and reversals

In fact,  $\mathcal{H}$  never keeps its equilibrium value,  $\bar{\mathcal{H}}$ , for a long time. Due to the stochastic ingredient in the turbulence model,  $\mathcal{H}$  fluctuates around the  $\bar{\mathcal{H}}$ -value. But as long as  $S$  and  $T$  remain close enough to  $\bar{S}$  and  $\bar{T}$ , large fluctuations of  $\bar{\mathcal{H}}$  are rare. In fact, the feedback mechanism succeeds in making  $S$ ,  $T$ , and  $\mathcal{H}$  to return to their steady values  $\bar{S}$ ,  $\bar{T}$ , and  $\bar{\mathcal{H}}$ . Fluctuations of  $S$  around  $\bar{S}$  can be seen as the secular variation of the model during a chron. But, due to the progressive population inversion described in detail in Narteau and Le Mouél (2005), it may happen that  $\mathcal{H}$  shows a large excursion toward positive or negative values. These extreme amplitudes of  $\mathcal{H}(t)$  do not depend on the intensity of the magnetic fields. In case of a positive  $\mathcal{H}$ -value, the linear system (Eqs. (2) and (3)) would have an unstable solution (the two eigenvalues are  $-K \pm \sqrt{\mathcal{H}\omega}$ , but the magnetic field reaction on the flow drives  $\mathcal{H}$  back to a smaller value, then  $S$ ,  $T$ , and  $\mathcal{H}$  towards  $\bar{S}$ ,  $\bar{T}$ , and  $\bar{\mathcal{H}}$ . In case of a negative  $\mathcal{H}$ -value, the solution  $(S, T)$  tends to  $(0, 0)$ . Indeed, the eigenvalues of the system are both real negative for  $0 < \mathcal{H} < 1/\omega\Theta^2$ , and complex conjugate with a negative real part  $(-K \pm i\sqrt{|\mathcal{H}|w})$  for  $\mathcal{H} < 0$ . As a consequence,  $S$  and  $T$  become weak, and the  $W$ -value decreases. When this value is low compared to the  $\bar{W}$ -value, oscillations of  $\mathcal{H}$  can be very rapid and large (Blanter et al., 1999), giving the chance for the system to recover its steady values with either the same polarity  $\bar{S}$ ,  $\bar{T}$ , and  $\bar{\mathcal{H}}$  (and thus accomplishing an excursion) or the opposite polarity  $-\bar{S}$ ,  $-\bar{T}$ , and  $-\bar{\mathcal{H}}$  (and thus accomplishing a reversal).

It is important to keep in mind that large negative excursions of  $\mathcal{H}$  do not happen with the same probability at any time during a chron. Indeed, a slow erosion in the dominance of cyclones with positive helicity which maintained the strength of the magnetic field is always happening during chrons. Large fluctuations of  $\mathcal{H}$  are observed only when this population inversion has been completed (Narteau and Le Mouél, 2005). Hence, after a reversal, negative excursions of  $\mathcal{H}$  are more likely to occur after a certain delay which is related to the efficiency of the population inversion mechanism (i.e. see the dependence of the  $E_0$ -value on the chron duration in Fig. 5a). Intuitively, the duration of this delay is the time required for the special configuration of the flow prevailing just after the reversal to wane.

The respective influence of the different parameters in generating various types of instabilities is illustrated by a schematic diagram in Fig. 2. A few kyr prior to a reversal – defined as the time when  $S$  crosses zero for the first time ( $t=0$  in Fig. 2) –  $\mathcal{H}$  starts decreasing, crosses the  $\bar{\mathcal{H}}$ -value, then zero, and accelerates its decay to finally reach and keep a minimum negative value for a few kyr. The generation term is negative in Eq. (3), and  $S$  decreases as soon as  $\mathcal{H} < 0$  and as long as  $T > 0$ . However  $T$  decreases when  $S < 0$  (Eq. (2)), and crosses zero. For a while both  $T$  and  $\mathcal{H}$  are  $< 0$ , and  $S$  increases; meanwhile,  $\mathcal{H}$  spontaneously changes sign and displays a large positive value (such a spontaneous symmetry

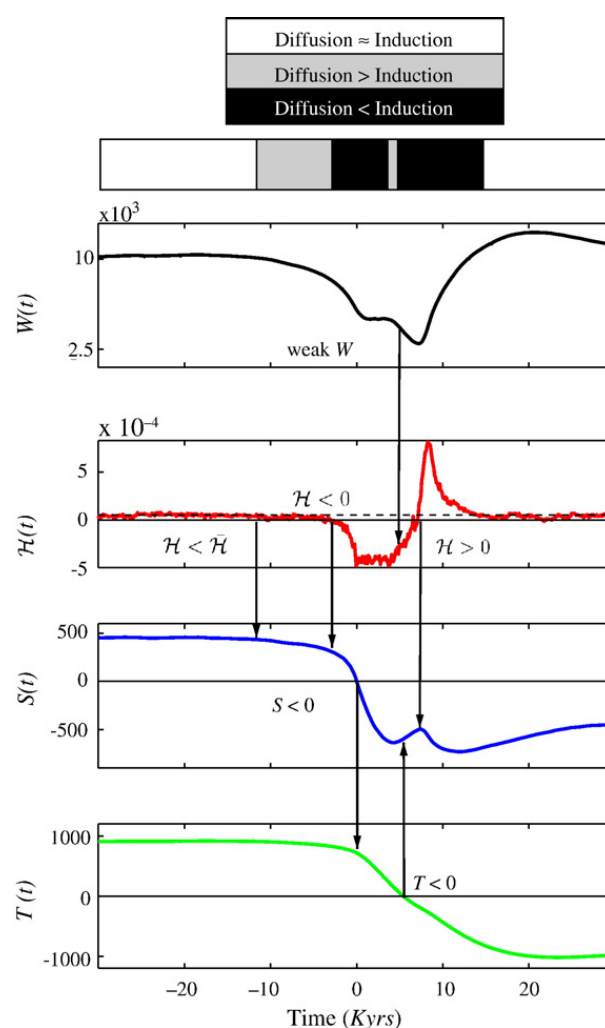


Fig. 2. Evolution of  $S$ ,  $T$ ,  $\mathcal{H}$ , and  $W$  during a reversal. These curves are obtained by averaging the behaviour of  $S$ ,  $T$ ,  $\mathcal{H}$ , and  $W$  over 300 simple reversals (Section 4.1 and Fig. 3). For each of them,  $t=0$  is the time at which  $S$  changes sign. The dashed line indicates the  $\bar{\mathcal{H}}$ -value. Arrows indicate a sequence of events that are causally related. At the top of the figure, a colorbar identifies the dominant mechanism: grey for the diffusion ( $S(t)\Theta^{-1}$  term in Eq. (3)), black for the induction ( $\mathcal{H}(t)T(t)$  term in Eq. (3)), white for the balance between diffusion and induction.

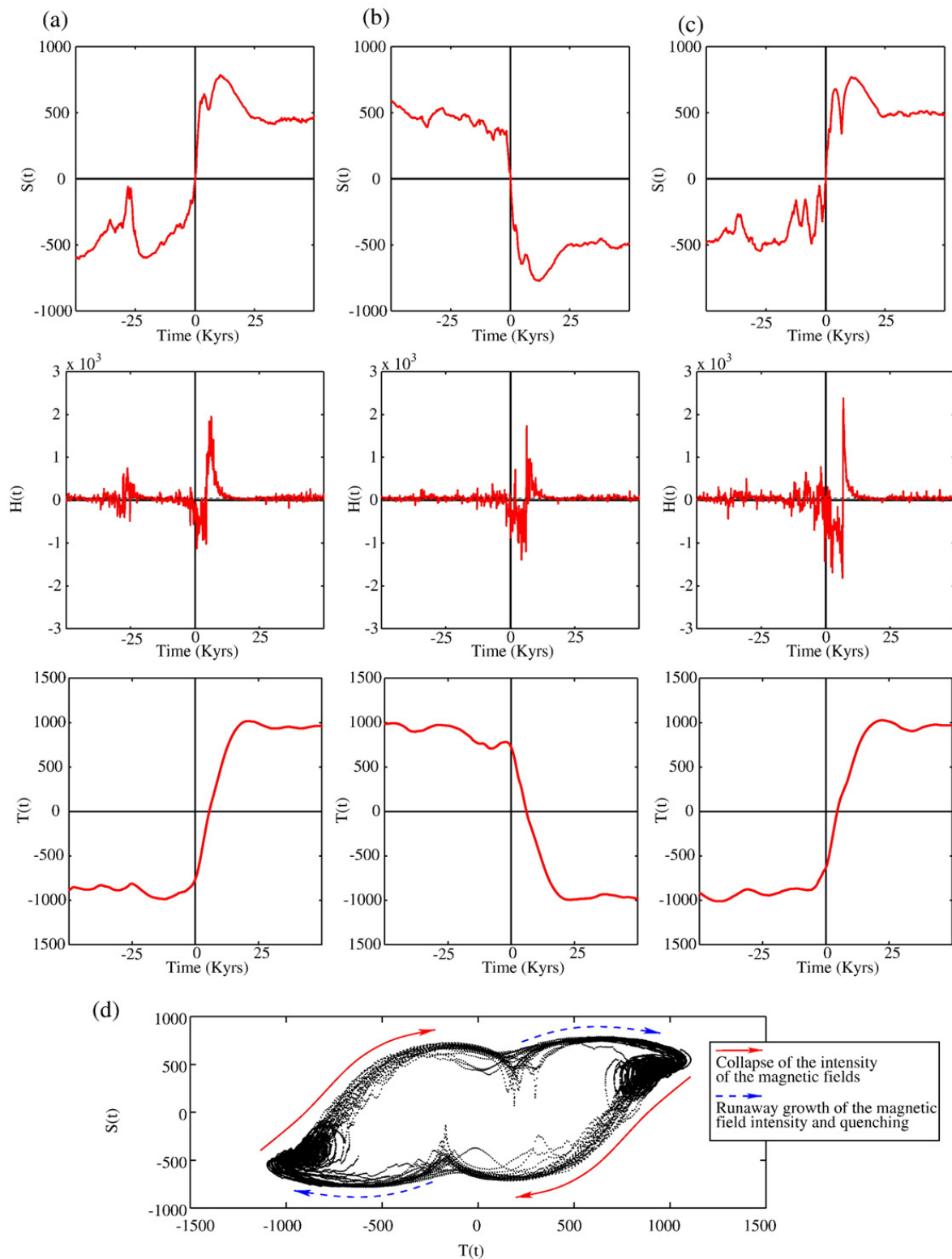


Fig. 3. Intensity and sign of the magnetic fields ( $S(t)$  and  $T(t)$ ) and the  $\alpha$ -effect ( $H(t)$ ) during three simple reversals (a), (b) and (c).  $t=0$  is the time of the reversal. Note the perfect synchronization between all these events. The dashed line  $\mathcal{H}(t) = K^2/\omega$  is the average  $\mathcal{H}$ -value during chrons. (d) Evolution of  $S(t)$  with respect to  $T(t)$  for a large number of rapid reversals.

breaking is described in details in Blanter et al. (1999)). Consequently,  $S$  decreases again in algebraic value, and shows an overshoot. Then,  $ST > 0$ ,  $H > 0$ ,  $S$  and  $T$  in-

crease in absolute value and the feedback mechanism is operating.  $\mathcal{H}$  retrieves its equilibrium value  $\bar{\mathcal{H}}$ , and  $S$  and  $T$  reach their  $\bar{S}$  and  $\bar{T}$ -values. Note that, as  $\bar{T} > \bar{S}$ ,

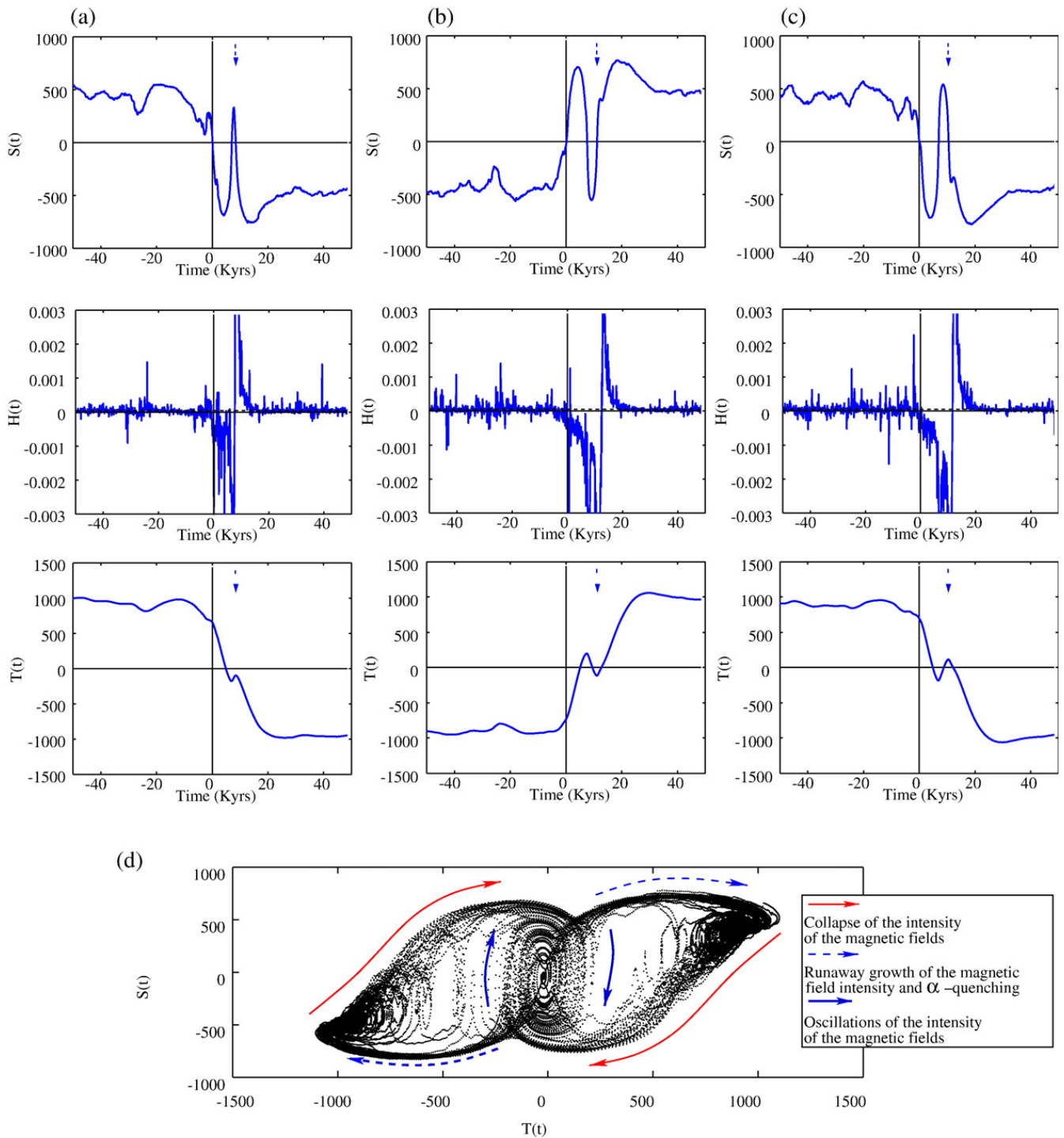


Fig. 4. Intensity and sign of the magnetic fields ( $S(t)$  and  $T(t)$ ) and the  $\alpha$ -effect ( $\mathcal{H}(t)$ ) during three unstable reversals (a), (b) and (c) characterized by more than one sign change of  $S(t)$ .  $t=0$  is the time of the reversal. Negative  $\mathcal{H}$ -values are associated with rapid changes of sign of  $S(t)$ . Dashed arrows indicate the time at which the stable polarity begins. The dashed line  $\mathcal{H}(t) = K^2/\omega$  is the average  $\mathcal{H}$ -value during chrons. (d) Evolution of  $S(t)$  with respect to  $T(t)$  for a large number of unstable reversals.

the main contribution to energy  $W$  is provided by the toroidal field, the retroaction mechanism on the flow weakens significantly only when  $T$  is small.

The behaviour depicted in Fig. 2 corresponds to a simple reversal, in which  $S$  crosses zero a single time. Reversals can present a more complex behaviour ac-

ording to the evolution of  $\mathcal{H}$ . After  $\mathcal{H}$  has decreased, changed sign and reached a negative value – which it keeps for a while, typically a few kyr, either it increases, changes sign and generally takes a large positive value, or it decreases again. The first case leads to a rapid reversal (Figs. 2 and 3), while the second is characterized by

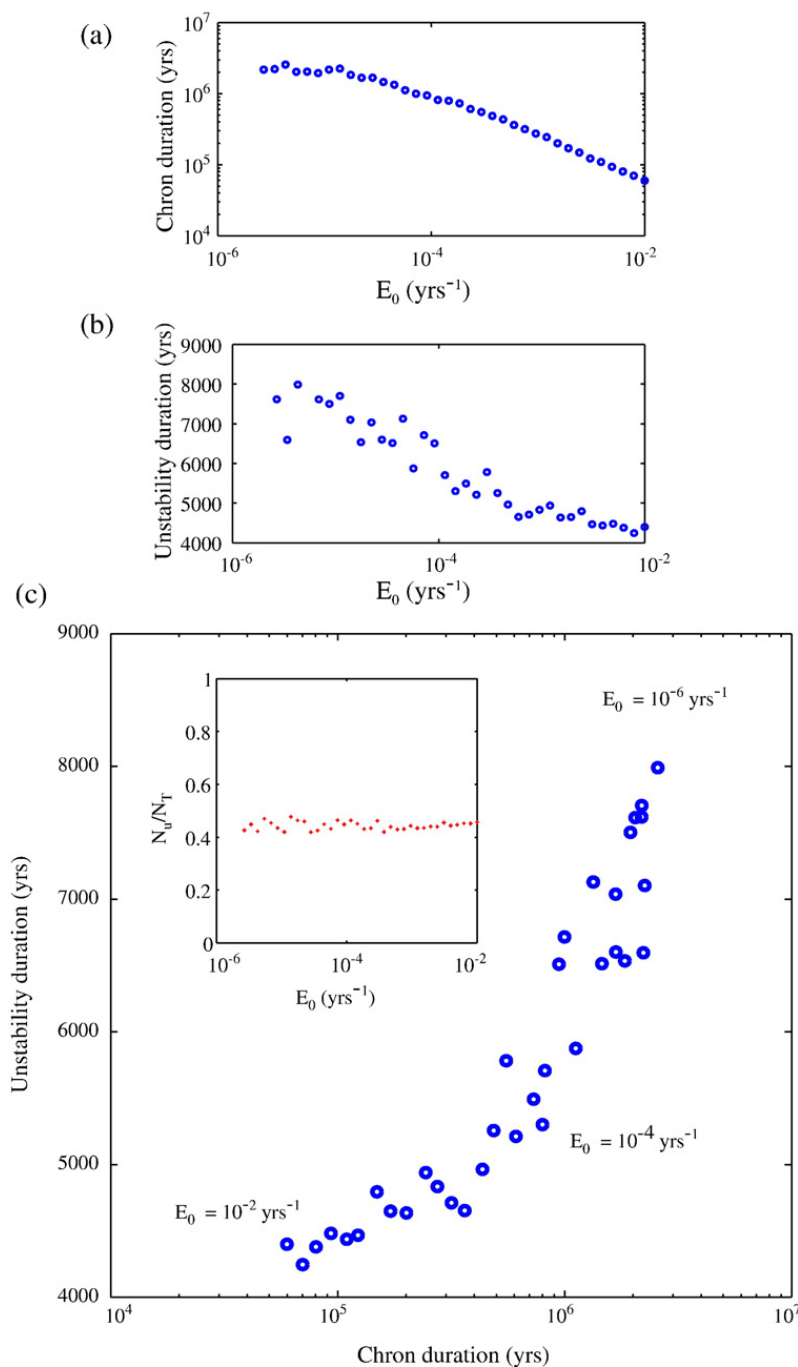


Fig. 5. (a) and (b) Evolution of the mean duration of the unstable state during reversals and the mean chron duration for  $E_0$  ranging from  $10^{-7}$  yr<sup>-1</sup> to  $10^{-2}$  yr<sup>-1</sup>. (c) Relationship between the mean duration of the unstable state during reversals and the mean chron duration. The inset shows the ratio between the number of unstable reversals  $N_u$  and the total number of reversals  $N_r$ .

successive oscillations (see unstable or more complex reversals in Fig. 4).

These two kinds of reversals are illustrated by few more examples in the following (Figs. 3 and 4).

#### 4.1. The phenomenology of reversals

Simple reversals are characterized by a single sign change of  $S$  (Figs. 2 and 3). Such reversals are observed

when  $\mathcal{H}$  is less than zero over a short period of time (no more than a few kyr) during the reversal. When  $\mathcal{H}$  becomes positive again,  $S$  has only changed sign one time,  $|S|$  increases and the solution returns to the opposite stationary state ( $\pm S$ ,  $\pm T$ ). Before the erosion process mentioned above, this event resets the original configuration of the flow similar to the onset of the previous chron (Narteau and Le Mouél, 2005). In Fig. 3 are shown examples representative of a few simple reversals.

More complex reversals can be characterized by more than one sign change of  $S$  (Fig. 4). After  $\mathcal{H}$  has become negative, there is a short time interval characterized by a large increase of negative cyclones. Then  $\mathcal{H}$  decreases again, enhancing the angular frequency ( $\sqrt{\mathcal{H}\omega}$ ) of the variations of the magnetic fields.  $|\mathcal{S}|$  continues decreasing, and crosses zero, before collapsing again when the toroidal field changes sign. This process can be repeated several times before a new spontaneous change of sign of  $\mathcal{H}$  restores a stable polarity, with either the same direction for an excursion, or the opposite one for a reversal. As for simple reversal the flow pattern is reset as it was at the beginning of the previous chron.

#### 4.2. Statistics of reversals

As mentioned in Section 2, helical forcing is symmetrical with respect to the sign of helicity. As a consequence, positive and negative changes of  $\mathcal{H}$  are equally probable after the field has collapsed ( $W \ll \bar{S}^2 + \bar{T}^2$ ). So, simple and more complex reversals are expected with the same probability over long times. The inset of Fig. 5 shows that this is indeed the case. The ratio of the number of unstable reversals to the total number of reversals in numerical experiments with parameter  $E_0$  varying over 4 orders of magnitude is always close to 0.5.

Over the same range of magnitudes of  $E_0$ , we estimated the average duration of more complex reversals (i.e. unstable reversals). The duration was defined as the time interval between the first and the last sign change of  $S$ , i.e. the time required to establish the new chron since the end of the previous one (Fig. 4, dashed lines). There is a positive correlation between the mean time  $\tau$ , i.e. the average duration of unstable reversals, and the average duration of chrons. When, from  $E_0 = 10^{-6} \text{ yr}^{-1}$  to  $E_0 = 10^{-2} \text{ yr}^{-1}$ , the mean chron duration varies by more than one order of magnitude, more precisely from 0.08 Myr to 2 Myr, the average duration of more complex reversals – or periods of instability – varies by a factor of two, from 4 to 8 kyr.

### 5. Testing the oscillatory behaviour of the geomagnetic field during reversals

It is interesting to test the phenomenological aspect predicted by the model for reversals versus paleomagnetic records. First, however, it must be stressed that such comparisons remains in essence limited to the field intensity since the model does not provide any indication of direction. Second, our knowledge also remains limited by the resolution and number of paleomagnetic

records. Although we will never reach a detailed and global description of the field variations during a reversal, the most detailed paleomagnetic records do provide first-order characteristics of the field variations during periods of stable polarity as well as during transitional periods. Sediments are rarely appropriate to document field behaviour during reversals since most records are associated with deposition rates in the order of a few centimeters per thousand years and thus unable to document rapid field changes. Sedimentary records are also hampered by some smearing of the field changes, which can affect a large part of the original signal. Only one very high resolution record (Channell et al., 2002) has been obtained from sediments which can somehow be compared with volcanic records. Because lava flows neither introduce any significant delay nor any smoothing in field recording, they appear to be much more suitable to properly document the reversal process rapidly, provided that a large number of flows recorded the transition.

Six volcanic records of reversals (Prévot et al., 1985; Herrero-Bervera et al., 1999; Herrero-Bervera and Valet, 1999; Coe et al., 2004; Riisager et al., 2004) have been obtained so far with enough intermediate directions to provide a reasonable description of the reversing field, and which satisfy specific conditions regarding their suitability (Valet and Herrero-Bervera, 2003). A dominant feature emerging from all six records is their complex structure, with large directional variations (particularly in inclination) immediately preceding and/or following the transition. The same behaviour is revealed by the most detailed record of the last reversal from sediments (Channell et al., 2002). Out of these six studies, only the Lower Mammoth (3.33 Ma) normal to reverse polarity transition (Herrero-Bervera and Valet, 2005) and the 15.5 Ma old reverse to normal Steens Mountains reversal (Prévot et al., 1985) incorporate paleointensity data and thus provide a description of the full vector. In Fig. 6 are shown these together with the variations in paleointensity and angular deviation, which represents the angle between the direction of the axial dipolar field at the site and the measured paleomagnetic vector, as a function of unit number. Note that the error bars on dating exceed typical durations of reversals, so that no detailed chronology of the events can be established with precision, but their succession is not questionable. During both reversals, we observe a synchronous oscillatory behaviour of intensity and field orientation. More specifically, the transitions are initiated by a complete change of polarity in the presence of a very weak field, followed by a short restoration to a higher intensity while remaining in the new polarity.

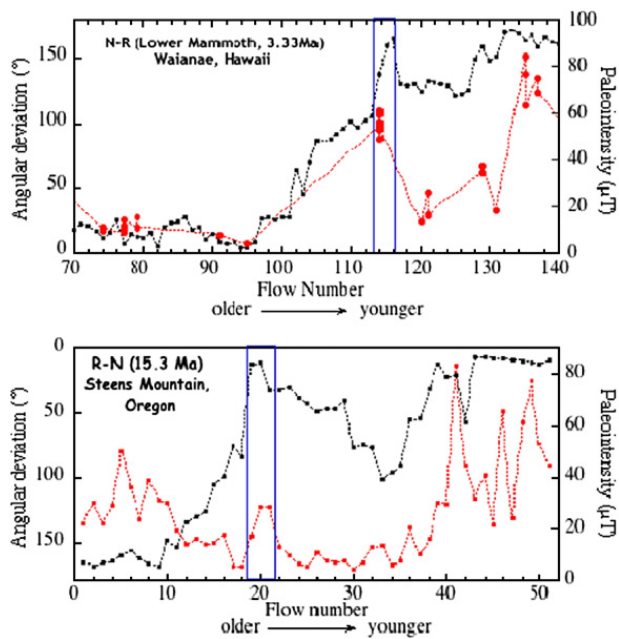


Fig. 6. Angular deviation and paleointensity during the lower Mammoth (top) and the Steens Mountains (bottom) reversals. In both cases, a synchronous oscillatory behaviour is observed: a maximum in intensity synchronizing with a full reversal of the orientation of the dipole (see the boxes); then, a minimum in intensity and a more unstable orientation of the geomagnetic field are observed before a stable polarity regime is reached.

However, the attempt to restore a dipolar configuration in the new polarity is unsuccessful and the field drops again and returns to a transitional configuration that is depicted by a large looping of the directions. The new polarity is finally reached and the reversal is completed by an intense field recovery which establishes a strong dipole field. As described above, large loops of the reversing vector prior to or after the switch between the two polarities are present in all the detailed records (Channell et al., 2002; Valet and Herrero-Bervera, 2003). Note also that transitional dipolar states have been reported in a few, although less detailed, records. These two datasets indicate that they are evidently linked and governed by the stability of the dipole. Similar behaviour has been reported in the case of the Réunion event (Carlut et al., 1999) with the absence of significant recovery between two successive rapid reversals. The final recovery of intensity during the ultimate stage of the transition has been observed in all volcanic records and does not depend on their resolution (Valet and Herrero-Bervera, 2007). It depicts another significant feature of the reversing field which is the asymmetry between very low field intensities prior to the transition, indicating low stability of the dipole, and very large strength of the field initiating the new polarity.

All these paleomagnetic observations are in agreement with the predictions of the multiscale dynamo model. Overall, a peak in intensity of the magnetic field during a reversal event should not be considered as an aborted chron, but rather as an expression of the possible oscillatory nature of the field during reversal.

## 6. Discussion and conclusion

We propose a conceptual model of turbulence in the presence of magnetic fields, which relies on a set of transitions in a hierarchical structure of length scales. Our intent here is to provide a phenomenological description of the basic features of the geodynamo using a simplified model with only two magnetic modes governed by two ordinary nonlinear differential equations. The originality of the model lies in the  $\mathcal{H}$  coefficient (Eq. (3)), which depends on the population of cyclones at each length scale of the hierarchical model. The cyclone population evolves according to the stochastic transitions which vary with the reaction of the magnetic field in the flow. In the presence of a weak field, the parameter  $\mathcal{H}$ , which is representative of the  $\alpha$ -effect, is subject to strong and rapid fluctuations.

The working regime of nonlinear dynamic systems often strongly varies with small changes in the governing parameter values, and the question of the generality of the results of the study should be addressed. In the two differential equations (Eqs. (2) and (3)) of our  $\alpha\omega$  dynamo model, there are two parameters,  $\Theta$  and  $\omega$ , the electromagnetic diffusion time and the zonal shear induction term due to differential rotation respectively. The value of the parameter  $\mathcal{H}$  results from the abstract model of turbulence and its steady value is given by formula (5) which evidences the feedback mechanism. So, when taking the turbulence model as it is,  $\omega$  is the unique control parameter that can be varied, but only in a reduced range (an order of magnitude of  $\omega$  in the Earth's case is easy to get). Practically, when varying  $\omega$  within an order of magnitude, all the model behaviours described above are conserved. But, in addition, the turbulence model has its own parameters. The main one is  $E_0$ . All the other parameter values are chosen in such a way that the model provides realistic time constants compared to the Earth magnetic fields and fluid mechanics experiments at a very high Rayleigh number (Niemela et al., 2000). Nevertheless, there is no qualitative change on the complete dynamo model when exploring, in a relatively unstructured manner, the influence of change by a few tens of percent of parameter values of the turbulence model variables.

The present study has been focused on field behaviour during reversals. This required to pay attention to the flow evolution during chrons, which is represented by populations of cyclones of different length scales. Due to the degradation of cyclones distribution, conditions for maintaining a statistically stationary flow become less and less favourable. In the meantime, the model exhibits a strong resilient character and permanently rebuilds a population distribution favourable to start a new chron. This results from a high variability of flow features when the magnetic field is weak.

According to the sign of the abrupt variation of helicity in the presence of weak magnetic fields, we found different degrees of complexity in reversal behaviours. It is shown, in the long run and over a large range of  $E_0$ -values, that the ratio between the number of rapid and unstable reversals is approximately the same. As shown in Section 2.1,  $E_0^{-1}$  is a fundamental time constant in the model. Both instability duration (or average duration,  $\tau$ , of more complex reversals, as defined above in Section 4.2), and chron duration increase with  $E_0$ , although rather slowly. The instability duration and the mean chron duration increase by a factor 2 and 20 respectively for  $E_0$  increasing by four orders of magnitude. This indicates that the time constants of the magnetic fields are not very sensitive to the time constant  $E_0^{-1}$ .

In fact, the diversity of reversal behaviour predicted by the model results from different patterns of interaction within the population of cyclones when the magnetic field intensity collapses during a preliminary phase of the reversal. Such a variability is only possible in models where the underlying equations/rules (e.g. the quenching mechanism of the  $\alpha$ -effect) do not causally uniquely determine the evolution of the system.

In our model, the configuration of the flow varies strongly. Such changes do not seem necessary to produce reversals in MHD numerical models (Christensen and Aubert, 2006). Nevertheless, in these models reversals are only observed in regimes where the dipole mode is extremely weak compared with other modes. More than the complete configuration of the flow, which is abstract in our model, a systematic measure of the correlation length of cyclonic activity could provide a link between the two approaches. It is significant that, in all cases, the propagation of instabilities is likely to be enhanced during reversals with respect to periods of stable polarity (chrons).

### Acknowledgements

The paper was improved by the constructive comments of J.J. Love and by thoughtful suggestions of

E. Herrero-Bervera and R. Hide. Clément Narteau benefits from a Marie Curie reintegration grant 510640-EVOROCK of the European Community and from a Specific Targeted Research Project of the European Community (12975-E2C2).

### References

- Blanter, E.M., Narteau, C., Shnirman, M.G., Le Mouél, J.-L., 1999. Up and down cascade in a dynamo model: spontaneous symmetry breaking. *Phys. Rev. E* 59, 5112–5123.
- Brandenburg, A., Krause, F., Meinel, R., Moss, D., Tuominen, I., 1989. The stability of non-linear dynamos and the limited role of kinematic growth rates. *Astron. Astrophys.* 213, 411–422.
- Carlut, J., Valet, J.-P., Quidelleur, X., Courtillot, V., Kidane, T., Gallet, Y., Gillot, P., 1999. Paleointensity across the Réunion event in Ethiopia. *Earth Planet. Sci. Lett.* 170, 17–34.
- Channell, J., Mazaud, A., Sullivan, P., Turner, S., Raymo, M., 2002. Geomagnetic excursions and paleointensities in the Matuyama chron at ocean drilling program sites 983 and 984 (Iceland basin). *J. Geophys. Res.* 107. doi:10.1029/2001JB000491.
- Chopard, B., Droz, M., 1998. *Cellular Automata Modeling of Physical Systems*. Cambridge University Press.
- Christensen, U., Aubert, J., 2006. Scaling properties of convection-driven dynamos in rotating spherical shells and application to planetary magnetic fields. *Geophys. J. Int.* 117, 97–114.
- Clement, B., 2004. Dependence of the duration of geomagnetic polarity reversals on site latitude. *Nature* 428, 637–640.
- Coe, R., Singer, B., Pringle, M., Zhao, X., 2004. Matuyama–Brunhes reversal and Kamikatsura event on Maui: Paleomagnetic directions,  $^{40}\text{Ar}/^{39}\text{Ar}$  ages and implications. *Earth Planet. Sci. Lett.* 222, 667–684.
- Dormy, E., Valet, J.-P., Courtillot, V., 2000. Numerical models of the geodynamo and observational constraints. *G<sup>3</sup>* 1, 2000GC000062.
- Frisch, U., Hasslacher, B., Pomeau, Y., 1986. Lattice-gas automata for the Navier–Stokes equation. *Phys. Rev. Lett.* 56 (14), 1505–1508.
- Glatzmaier, G.A., Roberts, P.H., 1995. A three-dimensional convective dynamo solution with rotating and finitely conducting inner core and mantle. *Phys. Earth Planet. Inter.* 91, 63–75.
- Herrero-Bervera, E., Valet, J.-P., 1999. Paleosecular variation during sequential geomagnetic reversals from Hawaii. *Earth Planet. Sci. Lett.* 171, 139–148.
- Herrero-Bervera, E., Valet, J., 2005. Absolute paleointensity from Hawaiian lavas younger than 35 ka. *Earth Planet. Sci. Lett.* 234, 279–296.
- Herrero-Bervera, E., Walker, G.P., Harrison, C., Guerrero Garcia, J., Kristjansson, L., 1999. Detailed paleomagnetic study of two volcanic polarity transitions recorded in eastern Iceland. *Phys. Earth Planet. Inter.* 115, 119–136.
- Hide, R., 1995. Structural instability of the Rikitake disk dynamo. *Geophys. Res. Lett.* 22, 1057–1059.
- Hide, R., 1998. Nonlinear quenching of current fluctuations in a self-exciting homopolar dynamo. *Nonlinear Process. Geophys.* 4, 201–205.
- Hoyng, P., Ossendrijver, M.A., Schmitt, D., 2001. The geodynamo as a bistable oscillator. *Geophys. Astrophys. Fluid Dyn.* 94, 263–314.
- Kageyama, A., Sato, T., 1997. Generation mechanism of a dipole field by a magnetohydrodynamic dynamo. *Phys. Rev., E* 55, 4617–4626.

- Kuang, W., Bloxham, J., 1997. An Earth-like numerical dynamo model. *Nature* 389, 371–374.
- Le Mouél, J.-L., Allègre, C.J., Narteau, C., 1997. Multiple scale dynamo. *Proc. Natl. Acad. Sci. U. S. A.* 94, 5510–5514.
- Narteau, C., Le Mouél, J., 2005. Transient evolution regimes in a multiscale dynamo model: timescales of the reversal mechanism. *J. Geophys. Res.* 110, B01104. doi:10.1029/2004JB002983.
- Narteau, C., Blanter, E.M., Le Mouél, J.-L., Shnirman, M.G., Allègre, C.J., 2000. Reversals sequences in a multiple scale dynamo mechanism. *Phys. Earth Planet. Inter.* 120, 271–287.
- Niemela, J.J., Skrnek, L., Sreenivasan, K.R., Donnelly, R.J., 2000. Turbulent convection at very high Rayleigh numbers. *Nature* 404, 837–840.
- Nozières, P., 1978. Reversals of the earth's magnetic field; an attempt at a relaxation model. *Phys. Earth Planet. Inter.* 174, 55–74.
- Olson, P., Christensen, U.R., Glatzmaier, G.A., 1999. Numerical modeling of the geodynamo: mechanisms of field generation and equilibration. *J. Geophys. Res.* 104, 10383–10404.
- Prévot, M., Mankinen, C., Coe, R., Grommé, C., 1985. The Steens Mountain (Oregon) geomagnetic polarity transition. Field intensity variations and discussion of reversal models. *J. Geophys. Res.* 90, 10417–10448.
- Quidelleur, X., 2003. The age and duration of the Matuyama–Brunhes transition from new K–Ar data from La Palma (Canary Islands) and revisited  $^{40}\text{Ar}/^{39}\text{Ar}$  ages. *Earth Planet. Sci. Lett.* 208, 149–163.
- Riisager, J., Riisager, P., Zhao, X., Coe, R., Pedersen, A., 2004. Paleointensity during a chron C26r excursion recorded in west Greenland lava flows. *J. Geophys. Res.* 109. doi:10.1029/2003JB002887.
- Rikitake, T., 1958. Oscillations of a system of disk dynamos. *Proc. Camb. Philos. Soc.* 54, 89–105.
- Simitev, R., Busse, F., 2005. Prandtl-number dependence of convection-driven dynamos in rotating spherical fluid shells. *J. Fluid Mech.* 435, 365–388.
- Stefani, F., Gerbeth, G., 2005. Asymmetric polarity reversals, bimodal field distribution, and coherence resonance in a spherically symmetric mean-field dynamo model. *Phys. Rev. Lett.* 94, 184506.
- Valet, J.-P., Herrero-Bervera, E., 2007. Geomagnetic reversals. In: Gubbins, D., Herrero-Bervera, E. (Eds.), *Encyclopedia of Geomagnetism and Paleomagnetism*, pp. 339–346.
- Valet, J.-P., Herrero-Bervera, E., 2003. Characteristics of geomagnetic reversals inferred from detailed volcanic records. *C. R. Acad. Sci. Paris* 335, 79–90.
- Valet, J., Meynadier, L., Guyodo, Y., 2005. Geomagnetic dipole strength and reversal rate over the past two million years. *Nature* 435, 802–805.